

# HIGH RESOLUTION NVD DIFFERENCING SCHEME FOR ARBITRARILY UNSTRUCTURED MESHES

H. JASAK<sup>a,\*</sup>, H.G. WELLER<sup>b</sup> AND A.D. GOSMAN<sup>b</sup>

<sup>a</sup> *Computational Dynamics Ltd., Olympic House, 317 Latimer Road, London W10 6RA, UK*

<sup>b</sup> *Department of Mechanical Engineering, Imperial College of Science, Technology and Medicine, London SW7 2BX, UK*

## SUMMARY

The issue of boundedness in the discretisation of the convection term of transport equations has been widely discussed. A large number of local adjustment practices has been proposed, including the well-known total variation diminishing (TVD) and normalised variable diagram (NVD) families of differencing schemes. All of these use some sort of an ‘unboundedness indicator’ in order to determine the parts of the domain where intervention in the discretisation practice is needed. These, however, all use the ‘far upwind’ value for each face under consideration, which is not appropriate for unstructured meshes. This paper proposes a modification of the NVD criterion that localises it and thus makes it applicable irrespective of the mesh structure, facilitating the implementation of ‘standard’ bounded differencing schemes on unstructured meshes. Based on this strategy, a new bounded version of central differencing constructed on the compact computational molecule is proposed and its performance is compared with other popular differencing schemes on several model problems. Copyright © 1999 John Wiley & Sons, Ltd.

KEY WORDS: convection discretisation; boundedness; unstructured meshes

## 1. INTRODUCTION

Discretisation of the convective part of fluid transport equations has proven to be one of the most troublesome parts of the numerical fluid mechanics. The objective is to devise a practice that will produce a bounded, accurate and convergent solution.

If one considers transport of scalar properties common in fluid flow problems, such as phase fraction, turbulent kinetic energy, species mass fractions, etc., the importance of boundedness becomes clear. For example, a negative value of turbulent dissipation in calculations involving  $k - \epsilon$  turbulence models results in negative turbulent viscosity, usually with disastrous effects on the solution algorithm. The convection term in its differential form does not violate the bounds of the variable given by its initial distribution. This property should, therefore, also be preserved in the discretised form of the term.

The analysis of basic differencing schemes in terms of Taylor series expansion [1] leads to the following conclusion:

---

\* Correspondence to: Computational Dynamics Ltd., Olympic House, 317 Latimer Road, London W10 6RA, UK. Tel.: +44 181 9699639; fax: +44 181 9688606; e-mail: h.jasak@cd.co.uk

- If the leading term of the truncation error includes odd-order spatial derivatives, the solution will be affected by a certain amount of numerical diffusion,
- If, on the other hand, the leading truncation term includes even-order derivatives, numerical dispersion occurs, causing unphysical and unbounded oscillations.

To make things worse, as is now well-known, only the first-order truncation of the Taylor series expansion (upwind differencing) guarantees the boundedness of the solution through the sufficient boundedness criterion. However, its first-order accuracy cannot be considered satisfactory. It has become obvious that a higher-order scheme needs to be non-linear (i.e. depend on the local shape of the solution) in order to be bounded and more than first-order-accurate at the same time [2].

The creation of a bounded convection differencing scheme can be divided into two parts:

- How to recognise the regions where intervention in the basic discretisation practice is needed; and
- What kind of intervention should be introduced.

In this paper, these issues in the context of the finite volume method (FVM) are considered, although the basic concepts also apply in other contexts.

Different procedures for assembling higher-order bounded differencing schemes have been suggested, the most popular being the total variation diminishing (TVD) [3–9] and the more recent group of normalised variable diagram (NVD) [1,10–12] approaches. All of these schemes introduce some procedure in which the discretisation practice for the convection term is adjusted locally, based on the currently available solution. In both families, the bounding procedure uses an indicator function that follows the local shape of the solution and is based on 1D analysis. Often the analysis refers to cells that are more than once removed from the face under consideration, usually in the ‘upwind’ direction [9,10].

One of the requirements of the differencing scheme presented in this paper is its applicability on unstructured meshes [13,14]. The convenience of mesh generation for such meshes makes them attractive for complicated geometries in industrial CFD applications. Arbitrarily unstructured meshing [15,16] further simplifies mesh generation in complicated geometries, but requires a more general face-based discretisation procedure (see e.g. [16,17]).

Only in hexahedral unstructured meshes is it possible to ‘recognise’ the distinct directions needed to implement the TVD and NVD-type schemes in 2D and 3D. In arbitrarily unstructured meshes, the concept of the ‘far upwind neighbour’ for a face becomes quite complicated. It is not clear how to determine the far neighbour since the mesh does not have any clear directionality (see Figures 1 and 2). For example, any of the points  $U_1$ ,  $U_2$  or even  $U_3$  in Figure 2 can be considered to be an appropriate choice of the far upwind node for the

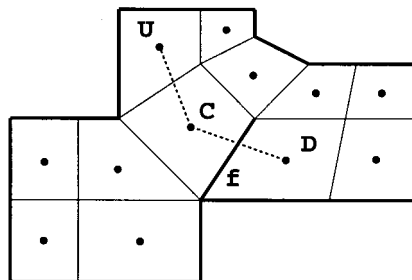


Figure 1. Unstructured quadrilateral mesh.

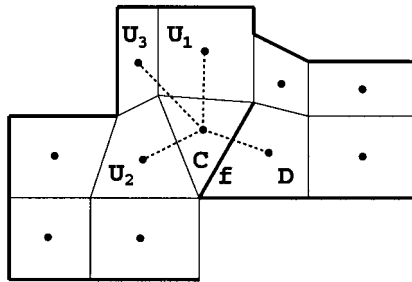


Figure 2. Arbitrarily unstructured mesh.

face  $f$ . The implementation of TVD- and NVD-type schemes in such circumstances is no longer a straightforward exercise. In fact, it has also become obvious that the directionality of the hexahedral mesh does not necessarily offer the appropriate ‘upwind’ information. On arbitrarily unstructured meshes, the problem is twofold: it is necessary to store the additional ‘far upwind’ addressing information (which is simply a programming issue) and, more importantly, determine which of the ‘upwind’ cells represents the right choice, which is neither simple nor unique. A more general definition of the unboundedness criterion that avoids the use of the ‘far upwind value’ is needed for both the TVD and NVD family of differencing schemes.

The Gamma differencing scheme described below is constructed bearing in mind the specific requirements of arbitrarily unstructured meshes. The test cases show that the proposed extension of the normalised variable approach (NVA) preserves the properties of the original formulation.

The rest of this paper will be divided into three parts. First, a general definition of the normalised variable, which is insensitive to mesh topology and spacing, will be presented. Using this new formulation, a novel form of bounded central differencing for both steady state and transient calculations will be presented<sup>1</sup>. Finally, a series of ‘standard’ test cases illustrating the behaviour of the differencing scheme will be shown for both structured and unstructured meshes.

## 2. CONVECTION BOUNDEDNESS CRITERION AND THE NVD DIAGRAM

The NVA and convection boundedness criterion (CBC) have been introduced by Leonard [10] and Gaskell and Lau [11]. Unlike the TVD approach [9], the NVA does not guarantee convergence of the proposed differencing scheme even in a 1D situation, but tackles the problem of boundedness in a more general way.

Consider the variation of a convected scalar  $\phi$  around the face  $f$  in a 1D case, Figure 3. The normalised variable is defined as [10]:

$$\tilde{\phi} = \frac{\phi - \phi_U}{\phi_D - \phi_U}, \quad (1)$$

where  $U$  and  $D$  refer to the points in Figure 3.

<sup>1</sup> One should have in mind that the new boundedness indicator is applicable for both the TVD and NVD differencing schemes on unstructured meshes, as any of the TVD limiters can be re-written in terms of the NVD boundedness indicator. A number of these limiters, as well as the general rules of ‘conversion’, can be found in [1].

With this definition, any differencing scheme using only the nodal values of  $\phi$  at points  $U$ ,  $C$  and  $D$  to evaluate the face value  $\phi_f$  can be written in the form:

$$\tilde{\phi}_f = f(\tilde{\phi}_C), \quad (2)$$

where

$$\tilde{\phi}_C = \frac{\phi_C - \phi_U}{\phi_D - \phi_U} \quad (3)$$

and

$$\tilde{\phi}_f = \frac{\phi_f - \phi_U}{\phi_D - \phi_U}. \quad (4)$$

In order to avoid unphysical oscillations in the solution, we will require that  $\phi_C$  (and consequently  $\phi_f$ ) are locally bounded between  $\phi_U$  and  $\phi_D$ , meaning either

$$\phi_U \leq \phi_C \leq \phi_D \quad (5)$$

or

$$\phi_U \geq \phi_C \geq \phi_D. \quad (6)$$

If this criterion is satisfied for every point in the domain, the entire solution will be free of any unphysical oscillations. This is the basis of the NVA.

The CBC [11] for  $\phi_C$  is given as:

$$0 \leq \tilde{\phi}_C \leq 1, \quad (7)$$

because by definition

$$\tilde{\phi}_C = 0 \Rightarrow \phi_C = \phi_U, \quad (8)$$

$$\tilde{\phi}_C = 1 \Rightarrow \phi_C = \phi_D. \quad (9)$$

Gaskell and Lau [11] show that the boundedness criterion for convection differencing schemes can be presented in the NVD, showing  $\tilde{\phi}_f$  as a function of  $\tilde{\phi}_C$ , as the hatched region in Figure 4 (including the line  $\tilde{\phi}_f = \tilde{\phi}_C$ ), or equivalently with the following conditions:

- For  $0 \leq \tilde{\phi}_C \leq 1$ ,  $\tilde{\phi}_f$  is bounded below by the function  $\tilde{\phi}_f = \tilde{\phi}_C$  and above by unity, and passes through the points  $(0, 0)$  and  $(1, 1)$ ,
- For  $\tilde{\phi}_C < 0$  and  $\tilde{\phi}_C > 1$ ,  $\tilde{\phi}_f$  is equal to  $\tilde{\phi}_C$ .

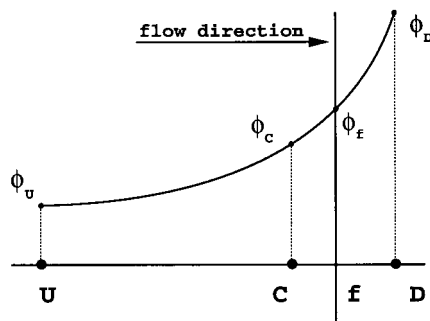


Figure 3. Variation of  $\phi$  around the face  $f$ .

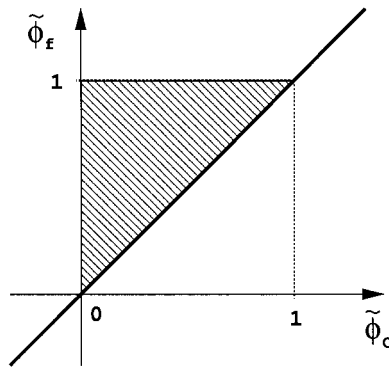


Figure 4. Convection boundedness criterion in the normalised variable diagram.

Figure 5 shows some basic differencing schemes in the NVD diagram: upwind differencing (UD), central differencing (CD), second-order linear upwind differencing (LUD) [18] and third-order QUICK [19]. It can be seen that the only basic differencing scheme that satisfies the boundedness criterion is UD. NVD diagrams for a number of TVD and NVD schemes, as well as the relationship between NVD and Sweby's diagram [9], can be found in [1].

The ULTIMATE NVD bounding strategy proposed by Leonard in [1] includes the dependence of the blending factor on the Courant number on the face. This is a consequence of the 'transient interpolation modelling' practice [1] included to compensate for the variation of the face value in time. While this enables a more accurate 1D modelling of transient phenomena, it presents a significant drawback in steady state situations, where the accuracy of the final solution depends on the size of the time step used to reach it, which is clearly undesirable. In the case of  $Co = 1$ , every differencing scheme using this strategy reduces to UD. In order to avoid this anomaly, the original form of the NVD diagram [11] illustrated in Figures 4 and 5 will be used.

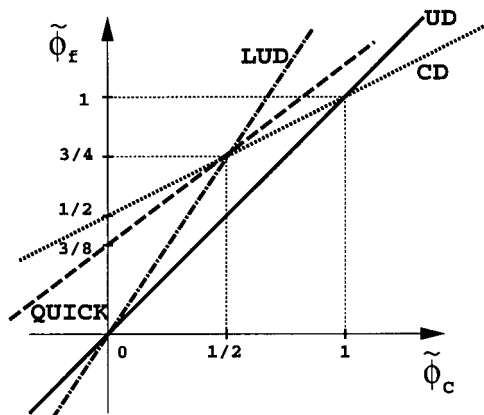


Figure 5. Some common differencing schemes in the NVD diagram.

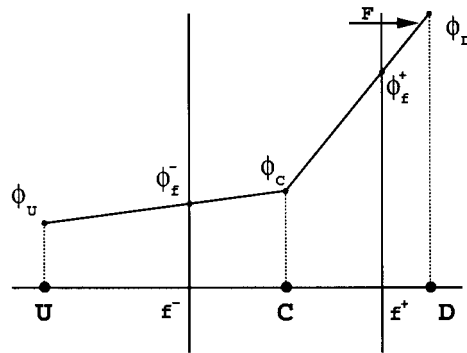


Figure 6. Modified definition of the boundedness criterion for unstructured meshes.

### 2.1. Modification of the NVD criterion for unstructured meshes

As can be seen in Equations (3) and (4), the CBC uses the value of the dependent variable  $\phi$  in the  $U$  (far upwind) node in order to determine  $\tilde{\phi}_C$ . This is not practical for arbitrarily unstructured meshes for reasons explained earlier.

A second issue to be considered is that the definition of the normalised variable, Equation (1), was originally given for a uniform mesh. This implies that a differencing scheme based on Equation (2) will be sensitive to sudden changes in the mesh spacing. A generalisation of the NVD criterion to non-uniform meshes has been given in [20]. However, this generalisation is complex and introduces additional computational cost.

In this section, a modification of the normalised variable in terms of gradients of the dependent variable will be presented. It enables the use of the NVA on arbitrarily unstructured and non-uniform meshes without an increase in computational cost.

Irrespective of the mesh structure, the information available for each cell face includes the gradients of the dependent variable over both cells sharing the face and the gradient across the face itself. If, as is usually the case, the computational point is located in the middle of the control volume, the definition of  $\tilde{\phi}_C$  can be changed in the following manner.

If the value of  $\phi_C$  is bounded by  $\phi_U$  and  $\phi_D$ , Figure 6, it is also bounded by the interpolated face values  $\phi_f^+$  and  $\phi_f^-$ . Advantage can be taken of this to base the calculation of the gradient of  $\phi$  across the cell on the interpolated face values, which is valid both on uniform and non-uniform meshes. The new definition of  $\tilde{\phi}_C$  is, therefore,

$$\tilde{\phi}_C = \frac{\phi_C - \phi_f^-}{\phi_f^+ - \phi_f^-} = 1 - \frac{\phi_f^+ - \phi_C}{\phi_f^+ - \phi_f^-}. \quad (10)$$

In the case of a uniform mesh, Equations (3) and (10) are equivalent.

The next step is to reformulate Equation (10) in terms of gradients across the face and the upwind cell  $C$  such that the 'far upwind node'  $U$  or the opposite face  $f^-$  are not explicitly used. For this purpose we shall consider a general polyhedral control volume around the point  $P$  and the neighbouring cell  $N$ , Figure 7. The face between  $P$  and  $N$  is marked with  $f$ . The correspondence between  $P$  and  $N$  with  $C$  and  $D$  from Figure 6 depends on the direction of the flux on the face  $f$ . If, for example, the flow leaves the cell through this face, it follows that  $P \equiv C$  and  $N \equiv D$ .

Using the interpolation factor  $f_x$ , defined as (see Figure 7):

$$f_x = \frac{\overline{fN}}{\overline{PN}}, \tag{11}$$

the difference  $\phi_f^+ - \phi_C$  can be written as

$$\phi_f^+ - \phi_C = f_x(\phi_D - \phi_C) = f_x \frac{\phi_D - \phi_C}{x_D - x_C} (x_D - x_C) = f_x (\nabla\phi)_f \cdot \hat{\mathbf{d}}(x_D - x_C), \tag{12}$$

since

$$\frac{\phi_D - \phi_C}{x_D - x_C} = (\nabla\phi)_f \cdot \hat{\mathbf{d}}. \tag{13}$$

Here,  $\hat{\mathbf{d}}$  is the unit vector parallel with  $\overline{CD}$  (or  $\overline{PN}$  in Figure 7),

$$\hat{\mathbf{d}} = \frac{\mathbf{d}}{|\mathbf{d}|}. \tag{14}$$

The transformation of  $\phi_f^+ - \phi_f^-$  can be done in the following way:

$$\phi_f^+ - \phi_f^- = \frac{\phi_f^+ - \phi_f^-}{x_f^+ - x_f^-} (x_f^+ - x_f^-) = (\nabla\phi)_C \cdot \hat{\mathbf{d}}(x_f^+ - x_f^-). \tag{15}$$

Using Equations (11), (12) and (15), the transformation of Equation (10) is simple:

$$\tilde{\phi}_C = 1 - \frac{\phi_f^+ - \phi_C}{\phi_f^+ - \phi_f^-} = 1 - \frac{f_x (\nabla\phi)_f \cdot \hat{\mathbf{d}}(x_D - x_C)}{(\nabla\phi)_C \cdot \hat{\mathbf{d}}(x_f^+ - x_f^-)}. \tag{16}$$

Since the computational point  $C$  is located in the middle of the cell, the following geometrical relation can now be used:

$$\frac{x_f^+ - x_f^-}{x_D - x_C} = 2 \frac{x_f^+ - x_C}{x_D - x_C} = 2f_x. \tag{17}$$

In multi-dimensions,  $f_x$  gives the estimate of the mesh grading in the direction of  $\mathbf{d}$ . For the other popular mesh arrangement, where the face  $f$  is half-way between  $P$  and  $N$  (which are not the centroids), a similar relationship can again be derived.

Combining Equations (16) and (17) yields:

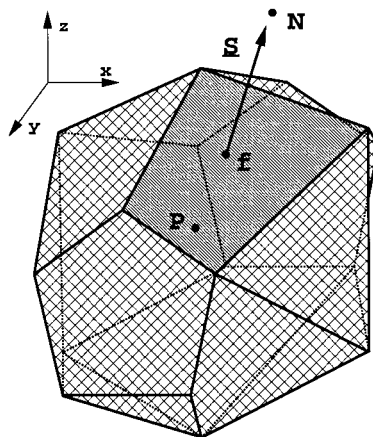


Figure 7. Control volume.

$$\tilde{\phi}_C = 1 - \frac{(\nabla\phi)_f \cdot \hat{\mathbf{d}}}{2(\nabla\phi)_C \cdot \hat{\mathbf{d}}} = 1 - \frac{(\nabla\phi)_f \cdot \mathbf{d}}{2(\nabla\phi)_C \cdot \mathbf{d}}, \quad (18)$$

where  $(\nabla\phi)_C$  is evaluated using, e.g. the discretised form of Gauss' theorem.

There is no reference to the 'far upstream' node  $U$ , or even to the opposite upstream face  $f^-$ . The product  $(\nabla\phi)_f \cdot \mathbf{d}$  is calculated directly from the values of the variable on each side of the face,

$$(\nabla\phi)_f \cdot \mathbf{d} = \phi_D - \phi_C, \quad (19)$$

and finally

$$\tilde{\phi}_C = 1 - \frac{\phi_D - \phi_C}{2(\nabla\phi)_C \cdot \mathbf{d}}. \quad (20)$$

Implementation of the NVD criterion on any mesh is now simple. The information about the topological structure of the mesh is irrelevant. Even the existence of the opposite face  $f^-$  is not required—it is only necessary to have the point  $C$  in the middle of the control volume. The formulation of  $\tilde{\phi}_C$  is now truly multi-dimensional: it can be calculated in the same way irrespective of the dimensionality of space, with the appropriate ( $n$ -dimensional) vectors  $\mathbf{d}$  and  $(\nabla\phi)_C$ . At the same time, on the cells with pairs of opposite faces, Equation (20) reduces exactly to Equation (10) (and indeed to Equation (3)).

### 3. GAMMA DIFFERENCING SCHEME

The above procedure allows the regions of the computational domain where an intervention in the basic discretisation practice is needed to be recognised, based on the NVD criterion. In this section, a basic higher-order differencing scheme will be selected, together with the interventions necessary to preserve the boundedness of the solution as prescribed by the NVA. The combination will be called the Gamma differencing scheme. The basic differencing scheme should be selected on the basis of its accuracy and consistency with the rest of the discretisation. Its unboundedness will be cured through the set of measures, depending on the local value of  $\tilde{\phi}_C$ .

The NVA family of schemes is based on a 1D analysis of the transport across the cell face. Although the extension to multi-dimensions is not obvious, it has regularly been implied, based on the extensive experience with other 1D boundedness criteria.

A popular choice of the basic differencing scheme seems to be the third-order upwind-biased QUICK [19], used in different ways in SMART [11], SHARP [10] and HLP [21]. This scheme is slightly unbounded and diffusive and is believed to need only a small modification to produce good results. The quadratic upwind interpolation used in QUICK, however, extends the computational molecule to include the second neighbours of the control volume, making it inconvenient for arbitrarily unstructured meshes. Having in mind that the overall accuracy of the finite volume method on arbitrarily unstructured meshes is usually second-order in space and time [16], it seems preferable to use the second-order central differencing (CD). This scheme uses a compact computational molecule, including only the nearest neighbours of the CV, making it practical for arbitrary mesh topologies.

CD is used unmodified wherever it satisfies the boundedness requirements. For the values of  $\tilde{\phi}_C < 0$  and  $\tilde{\phi}_C > 1$ , the boundedness criterion prescribes the use of UD in order to guarantee boundedness. Therefore, some sort of 'switching' between the schemes is needed. This causes the most serious problem related to the family of NVD differencing schemes: the perturbations



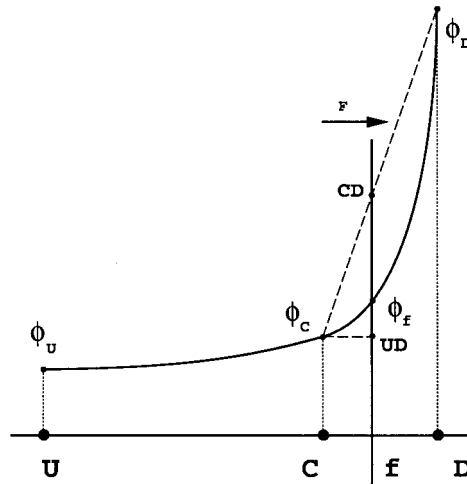


Figure 8. Shape of the profile for  $0 < \tilde{\phi}_C < \beta_m$ .

introduced by switching within the discretisation practice often cause an instability in the calculation, sometimes preventing convergence. In order to overcome this difficulty, the majority of existing NVD schemes use a form of linear upwinding in the range of values  $0 < \tilde{\phi}_C < \beta_m$ , where  $\beta_m$  is a constant of the differencing scheme, usually around  $\frac{1}{6}$  [11]. The meaning of  $\beta_m$  will become clear from further discussion (see Section 3.1).

Values of  $\tilde{\phi}_C$  close to 0 ( $\tilde{\phi}_C > 0$ ) imply a profile of the dependent variable similar to the one shown in Figure 8, where a smooth variation of  $\phi$  between  $U$  and  $C$  is followed by a sharp change between  $C$  and  $D$ . If the curve passing through  $\phi_U$ ,  $\phi_C$  and  $\phi_D$  is regarded as the exact form of the bounded local profile, it can be seen that the exact face value  $\phi_f$  is bounded by the values obtained from UD and CD. It follows that some kind of blending between the two can be used to obtain a good estimate of the face value.

In order to establish a smooth transition, the blending between UD and CD should be used smoothly over the interval  $0 < \tilde{\phi}_C < \beta_m$  and the blending factor  $\gamma$  should be determined on the basis of  $\tilde{\phi}_C$ , such that:

- $\tilde{\phi}_C = 0 \Rightarrow \gamma = 0$  (upwind differencing),
- $\tilde{\phi}_C = \beta_m \Rightarrow \gamma = 1$  (central differencing).

This practice simultaneously satisfies two important requirements:

- The face value in situations of rapidly changing derivative of the dependent variable is well-estimated and a smooth change in gradients is secured. This has proven to be much better than forms of the linear upwinding usually used in this situation [11,12].
- The transition between UD and CD is smooth. This reduces the amount of switching in the differencing scheme and improves convergence. In other NVD schemes there is a point where a small change in the value of  $\tilde{\phi}_C$  causes an abrupt change in the computational molecule, causing deterioration in convergence. With the present differencing scheme, this is not the case.

The blending factor  $\gamma$  has been selected to vary linearly between  $\tilde{\phi}_C = 0$  and  $\tilde{\phi}_C = \beta_m$  according to:

$$\gamma = \frac{\tilde{\phi}_C}{\beta_m}. \quad (21)$$

The proposed Gamma differencing scheme thus operates as follows:

- For all the faces of the mesh, check the direction of the flux and calculate:

$$\tilde{\phi}_C = \frac{\phi_C - \phi_U}{\phi_D - \phi_U} = 1 - \frac{\phi_D - \phi_C}{2(\nabla\phi)_C \cdot \mathbf{d}} \quad (22)$$

from the previous available solution or the initial guess.

- Based on  $\tilde{\phi}_C$ , calculate  $\tilde{\phi}_f$  as:
  - for  $\tilde{\phi}_C \leq 0$  or  $\tilde{\phi}_C \geq 1$  use UD:

$$\tilde{\phi}_f = \tilde{\phi}_C \Rightarrow \phi_f = \phi_C, \quad (23)$$

- for  $\beta_m \leq \tilde{\phi}_C < 1$  use CD:

$$\tilde{\phi}_f = \frac{1}{2} + \frac{1}{2} \tilde{\phi}_C, \quad (24)$$

or, in terms of unnormalised variables:

$$\phi_f = f_x \phi_C + (1 - f_x) \phi_D, \quad (25)$$

- for  $0 < \tilde{\phi}_C < \beta_m$  blending is used:

$$\tilde{\phi}_f = -\frac{\tilde{\phi}_C^2}{2\beta_m} + \left(1 + \frac{1}{2\beta_m}\right) \tilde{\phi}_C, \quad (26)$$

or, in terms of unnormalised variables:

$$\phi_f = (1 - \gamma(1 - f_x)) \phi_C + \gamma(1 - f_x) \phi_D. \quad (27)$$

The blending factor  $\gamma$  is calculated from the local value of  $\tilde{\phi}_C$  and the pre-specified constant of the scheme,  $\beta_m$ , Equation (21).

The NVD diagram for this differencing scheme is shown in Figure 9.

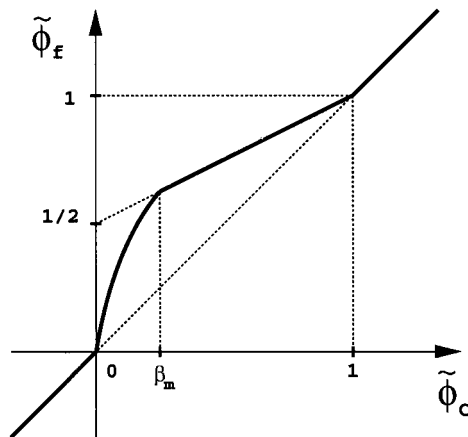


Figure 9. Gamma differencing scheme in the NVD diagram.

### 3.1. Accuracy and convergence of the Gamma differencing scheme

The role of the  $\beta_m$  coefficient can be seen in Figure 9—the larger the value of  $\beta_m$ , the more blending will be introduced. At the same time, the transition between UD and CD will be smoother. For good resolution, the value of  $\beta_m$  should ideally be kept as low as possible.

An upper limit on  $\beta_m$  comes from the accuracy requirement. For  $\bar{\phi}_C = \frac{1}{2}$  the variation of  $\phi$  is linear between  $U$  and  $D$  and CD reproduces the exact value of  $\phi_f$ :  $\beta_m$  should, therefore, always be less than  $\frac{1}{2}$ . Higher values of  $\beta_m$  result in more numerical diffusion. For good resolution of sharp profiles,  $\beta_m$  should ideally be kept to about  $\frac{1}{10}$ . Lower values do not improve the accuracy, but introduce the ‘switching’ instability. The useful range of  $\beta_m$  is therefore:

$$\frac{1}{10} \leq \beta_m \leq \frac{1}{2}. \quad (28)$$

The other factor influencing the choice of  $\beta_m$  is the convergence for steady state calculations. The non-convergence of the NVD-type schemes presents itself as the inability to reduce the residual to an arbitrary low level, which, however, does not impair the quality of the solution: one discretisation error (previously visible as either unboundedness or numerical diffusion) has been transformed into another (residual) and it is up to the user to determine the desired balance between the two.

The problem of convergence with the Gamma differencing scheme is less serious than with other schemes of the switching type because of the smooth transition between UD and CD. A universal remedy for convergence problems is to increase the value of  $\beta_m$  (but not over  $\frac{1}{2}$ ), effectively allowing the user to choose between the acceptable level of numerical diffusion and the convergence error.

Unlike the ULTIMATE NVD limiter [1], the face value of  $\phi$  in the Gamma differencing scheme is not dependent on the Courant number. Steady state solutions will, therefore, be independent of the size of the time step or the relaxation factor used to reach it.

## 4. TEST CASES

In this section we shall present two groups of test cases. Section 4.1 concentrates on the ‘standard’ resolution tests on regular structured meshes designed to compare the accuracy of the new differencing scheme against some established schemes of similar type. The second group of test cases, Section 4.2, are for unstructured meshes, where a strict implementation of the TVD or NVD criterion was previously impossible.

### 4.1. Resolution tests

The tests to be presented here show that the Gamma differencing scheme with  $\beta_m$  set to 0.1 exhibits the following properties:

- In the cases with smoothly changing gradients of the dependent variable the scheme behaves like central differencing.
- In the cases with sharp gradients it gives the sharp resolution of central differencing, eliminating at the same time any unphysical oscillations in the solution.

The first set of cases all pertain to a steady state convection of a scalar  $\phi$ , Equation (29), in a square domain shown in Figure 10:

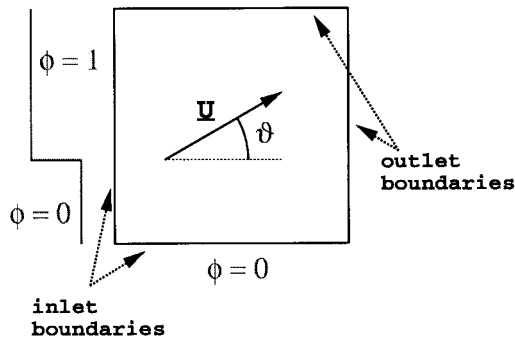


Figure 10. Step profile test set-up.

$$\nabla \cdot (\mathbf{U}\phi) = 0. \quad (29)$$

The mesh consists of  $30 \times 30$  uniformly spaced CVs and the comparison of the profiles on the line parallel with the inlet, 20 CVs downstream from the left boundary will be presented. The mesh-to-flow angle is fixed to  $30^\circ$ .

Following Leonard [1], three inlet boundary profiles of  $\phi$  are selected:

- Step profile:

$$\phi(x) = \begin{cases} 0 & \text{for } 0 \leq x < \frac{1}{6}, \\ 1 & \text{for } \frac{1}{6} \leq x \leq 1, \end{cases} \quad (30)$$

- $\sin^2$  profile:

$$\phi(x) = \begin{cases} \sin^2[3\pi(x - \frac{1}{6})] & \text{for } \frac{1}{6} \leq x < \frac{1}{2}, \\ 0 & \text{elsewhere,} \end{cases} \quad (31)$$

- Semi-ellipse:

$$\phi(x) = \begin{cases} \sqrt{1 - \left(\frac{x - \frac{1}{3}}{\frac{1}{6}}\right)^2} & \text{for } \frac{1}{6} \leq x < \frac{1}{2}, \\ 0 & \text{elsewhere.} \end{cases} \quad (32)$$

The differencing schemes included in this comparison are:

- Gamma scheme, Section 3,
- Self-filtered central differencing (SFCD) [22],
- van Leer TVD scheme [7],
- SUPERBEE–TVD scheme by Roe [6],
- SOUCUP–NVD scheme by Zhu and Rodi [23],
- SMART–NVD scheme by Gaskell and Lau [11].

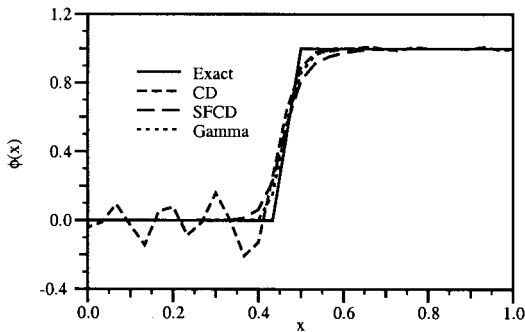
*4.1.1. Step profile.* The results for the first test case are shown in Figure 11. Several interesting features can be recognised. The Gamma differencing scheme gives the resolution of CD over the step and completely removes unphysical oscillations. The step resolution for Gamma is far superior to the older version of stabilised central differencing (SFCD).

SUPERBEE, Figure 11(b), actually gives better step resolution than Gamma. This is the most compressive TVD differencing scheme. While SUPERBEE is very good for sharp profiles, it also tends to artificially sharpen smooth gradients [1].

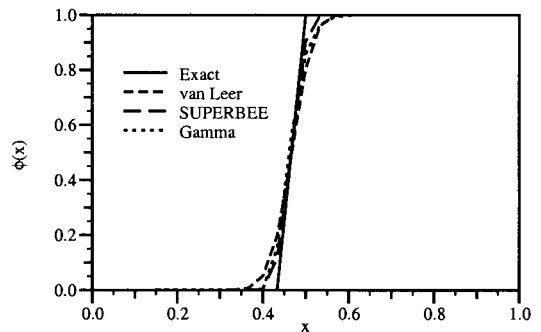
SOUCUP, Figure 11(c), is more diffusive than Gamma. The other NVD scheme, SMART, gives a solution very close to the one obtained from the Gamma differencing scheme. One should have in mind that SMART is actually a stabilised version of QUICK [19] and uses a computational molecule which is twice the size of the one used by CD and Gamma.

4.1.2. *sin<sup>2</sup> profile.* The results for the convection of a sin<sup>2</sup> profile are shown in Figure 12. This test case has been selected to present the behaviour of the differencing schemes on smoothly changing profiles. Another interesting feature of this test is a one-point peak in the exact solution, Figure 12(a). It is known that TVD schemes reduce to first-order accuracy in the vicinity of extreme. This phenomenon is usually called ‘clipping’. The amount of ‘clipping’ gives us a direct indication of the quality of the differencing scheme.

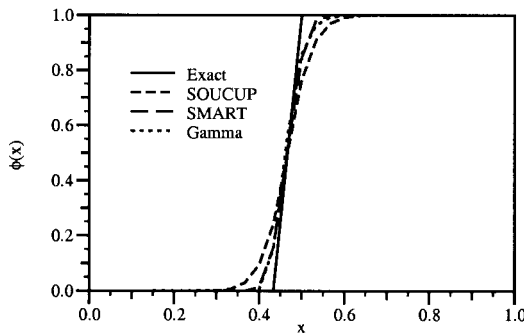
SFCD, Figure 12(a), shows a considerable amount of ‘clipping’. The maximum of the profile for the Gamma differencing scheme is about 0.85—considerably less than that for CD. This is the price that needs to be paid for a bounded solution.



(a) CD, SFCD and Gamma schemes.

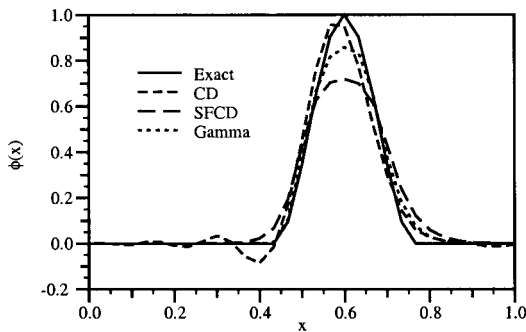


(b) Van Leer, SUPERBEE and Gamma schemes.

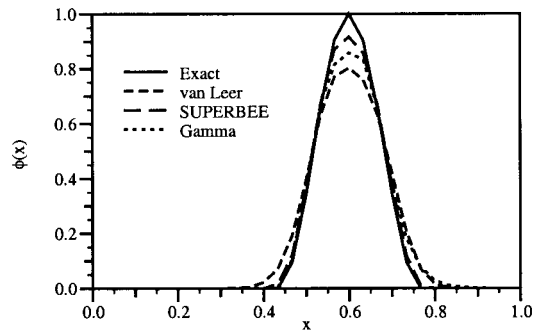


(c) SOUCUP, SMART and Gamma schemes.

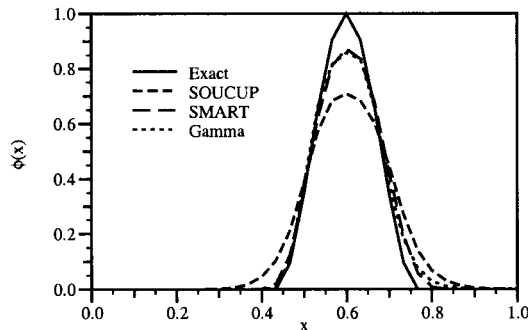
Figure 11. Convection of a step profile,  $\theta = 30^\circ$ .



(a) CD, SFCD and Gamma schemes.



(b) Van Leer, SUPERBEE and Gamma schemes.



(c) SOUCUP, SMART and Gamma schemes.

Figure 12. Convection of a  $\sin^2$  profile,  $\theta = 30^\circ$ .

The best of the TVD schemes is again SUPERBEE, Figure 12(b). It follows the exact profile quite accurately and peaks at about  $\phi = 0.9$ . The van Leer TVD limiter still seems to be too diffusive.

Figure 12(c) shows the comparison for the NVD schemes. Again, there is not much difference between SMART and Gamma solutions. SOUCUP still seems to be too diffusive.

**4.1.3. Semi-ellipse.** The results for the convection of a semi-elliptic profile with the selected differencing schemes are shown in Figure 13. The main feature of this test-case is an abrupt change in the gradient on the edges of the semi-ellipse, followed by the smooth change in  $\phi$  over the elliptic part. The CD scheme, Figure 13(a), introduces oscillations in the solution within the smooth region of the real profile. This is usually called ‘waviness’ [1]. Gamma again proves to be a more effective way of stabilising CD than SFCD.

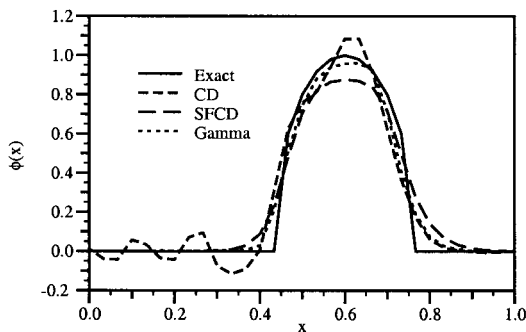
Figure 13(b) shows the problems with SUPERBEE—it tries to transform the semi-ellipse into a top-hat profile, as has been noted by Leonard [1]. Van Leer’s limiter performs quite well in this situation. This can be attributed to the balanced introduction of numerical diffusion and anti-diffusion used in this limiter. Gamma, on the other hand, loses the symmetry seen in the real profile.

The solutions for SMART and Gamma, Figure 13(c) are again quite close; SMART gives marginally smaller ‘clipping’ of the top and Gamma follows the smooth part of the profile better. SOUCUP, while describing the smooth profile well, clips off about 10% of the peak

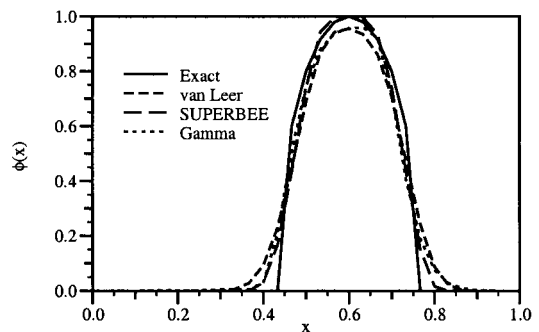
4.2. Unstructured meshes

We shall now present three examples illustrating the behaviour of the new differencing scheme on unstructured meshes. For this purpose, the step profile test problem described in Section 4.1.1 has been solved on a mesh consisting of uniform hexagons (in a honeycomb configuration) and on a mesh of triangles created by splitting each hexagon into six equal parts. This configuration has been selected to minimise the effects of directionality present in the triangular meshes obtained by splitting a mesh of squares. The details of both meshes are given in Figure 14.

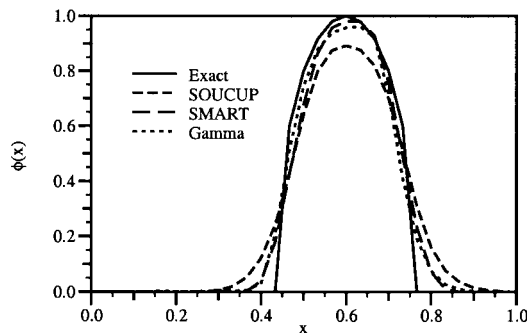
Results for three differencing schemes will be presented: UD, CD and the Gamma scheme. Other TVD and NVD schemes can also be implemented on unstructured meshes if the limiter in question is described in terms of NVA and Equation (20) is used to calculate  $\tilde{\phi}_C$ . As the



(a) CD, SFCD and Gamma schemes.



(b) Van Leer, SUPERBEE and Gamma schemes.



(c) SOUCUP, SMART and Gamma schemes.

Figure 13. Convection of a semi-ellipse,  $\theta = 30^\circ$ .

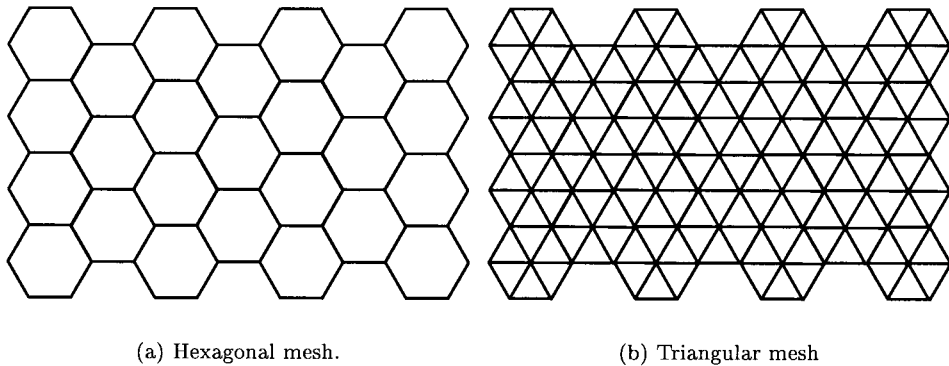


Figure 14. Regular unstructured meshes.

purpose of the tests presented below is to demonstrate the behaviour of the convection discretisation on unstructured meshes they have been omitted for the sake of brevity.

**4.2.1. Hexagonal mesh.** Strictly speaking, the mesh of hexagons contains pairs of opposite faces on each control volume, but unlike the quadrilateral meshes, the three mesh 'directions' are not orthogonal. This removes the possibility of compensation of the discretisation error present in quadrilateral meshes. This example is included to demonstrate that Equation (20) can be used on meshes consisting of control volumes of arbitrary polyhedral shape.

Figure 15 shows the solution for the three differencing schemes under consideration. CD, Figure 15(b), again produces an unbounded solution with strongly pronounced waviness, which is successfully removed by the Gamma limiter, Figure 15(c). It can also be seen that the step-resolution is inferior to the one on the quadrilateral mesh (Figure 11(a)).

**4.2.2. Triangular mesh.** Unlike the above example, a mesh of triangles does not possess a set of 'opposite' faces and, therefore, represents a more searching test of the extension of the NVD criterion.

Figure 16 shows the comparison between UD, CD and Gamma results on the triangular mesh. It can be seen that even in this situation the Gamma scheme successfully removes the oscillations present in the CD solution, while preserving the sharpness of the profile. It is also interesting to notice that the oscillations in the CD solution show less regularity than on the mesh of squares, Figure 11(a).

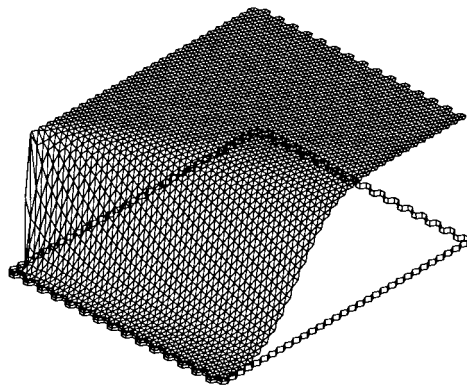
**4.2.3. Arbitrarily unstructured mesh, supersonic flow.** The final test of the differencing scheme will be done on an arbitrarily unstructured mesh, consisting of control volumes of different topology generated by locally subdividing an originally quadrilateral mesh. Here, the case of an inviscid Mach 3 supersonic steady flow of a perfect gas over a forward-facing step is calculated.

For the details of the pressure-based supersonic flow algorithm used in this calculation, the reader is referred to [24]. Here, it will only be mentioned that the set of equations contains three convection terms. Two of them are the 'conventional' terms, appearing in the momentum and energy equations, and the third represents the redistribution of the density by the sonic velocity in the equation for the pressure. In this case it is essential to preserve the boundedness, as the negative values of temperature would produce negative density, with disastrous effects on the convergence.

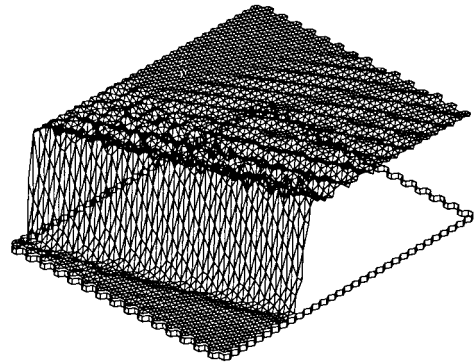


The mesh used for this calculation is a result of automatic adaptive refinement algorithm of an initially quadrilateral mesh. The refinement algorithm splits the original cell into four and propagates the refinement patterns through the mesh until a regularity condition is satisfied. The detail of the mesh is shown in Figure 17. It consists of control volumes that are either quadrilateral or pentagonal in topology; the ‘hanging nodes’ on the interfaces between smaller and larger cells are treated in a manner described in [14,17]. The details of the refinement procedure as well as the formulation of the error estimate used to produce the mesh can be found in [16].

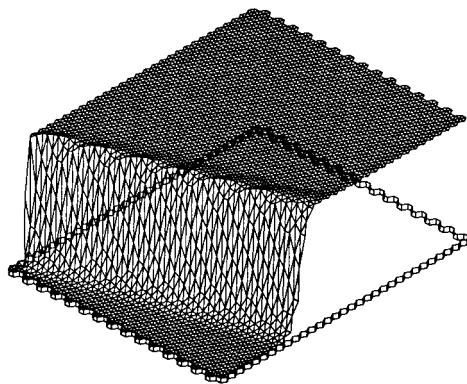
The Gamma differencing scheme has been used on all convection terms. The resulting Mach number distribution is shown in Figure 18. It can be seen that a combination of adaptive refinement and the Gamma scheme produces excellent shock resolution while preserving the necessary boundedness of the solution.



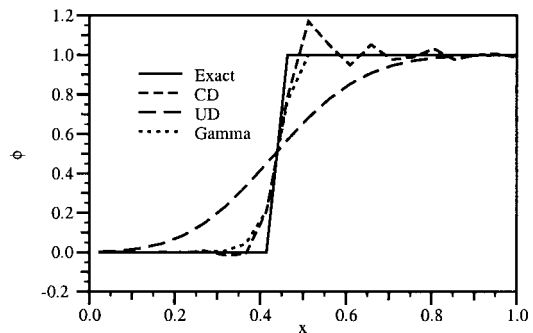
(a) Upwind differencing.



(b) Central differencing.



(c) Gamma scheme.



(d) Comparison of profiles.

Figure 15. Convection of a step profile on the mesh of hexagons.

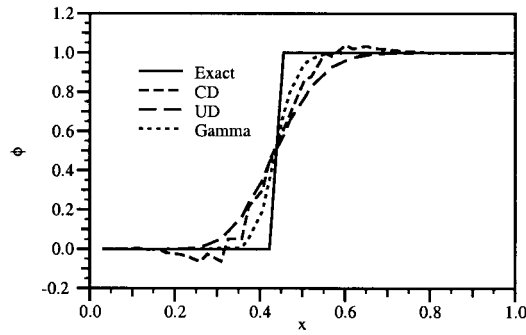


Figure 16. Convection of a step profile on the mesh of triangles.

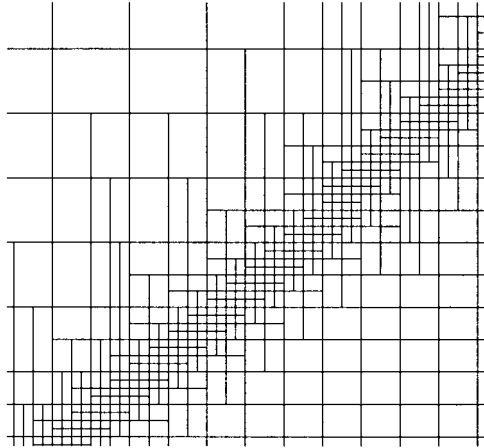


Figure 17. Supersonic flow: detail of the mesh.

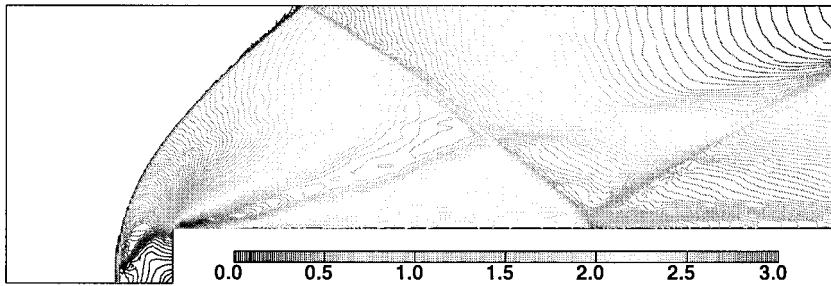


Figure 18. Mach number distribution.

## 5. SUMMARY

The first part of this paper describes the modification of the smoothness indicator used in conjunction with the NVA, allowing the implementation of the NVD family of bounded differencing schemes on unstructured meshes. The new form of  $\tilde{\phi}_C$  does not explicitly use the 'far upwind node' value and takes into account non-uniform mesh spacing.

In the second part, the NVD-based Gamma differencing scheme is introduced as a bounded form of CD, which uses only the compact computational molecule. The test cases presented in

Section 4 show that the performance of the differencing scheme is comparable with that of more popular versions of bounded QUICK and better than the older versions of bounded CD and two popular TVD limiters. Finally, several unstructured mesh examples have been presented, including the mesh of triangles and hexagons as well as an arbitrarily unstructured mesh, which show that the proposed modification is performed well, independently of the mesh structure.

## REFERENCES

1. B.P. Leonard, 'The ULTIMATE conservative difference scheme applied to unsteady one-dimensional advection', *Comp. Methods Appl. Mech. Eng.*, **88**, 17–74 (1991).
2. C. Hirsch, *Numerical Computation of Internal and External Flows*, Wiley, New York, 1991.
3. S. Osher and S.R. Chakravarthy, 'High resolution schemes and the entropy condition', *SIAM J. Numer. Anal.*, **21**, 955–984 (1984).
4. A. Harten, 'High resolution schemes for hyperbolic conservation laws', *J. Comp. Phys.*, **49**, 357–393 (1983).
5. A. Harten, 'On a class of high resolution total variation stable finite difference schemes', *SIAM J. Numer. Anal.*, **31**, 1–23 (1984).
6. P.L. Roe, 'Large scale computations in fluid mechanics, part 2', in *Lectures in Applied Mathematics*, vol. 22, Springer, Berlin, 1985, pp. 163–193.
7. B. Van Leer, 'Towards the ultimate conservative differencing scheme. II Monotonicity and conservation combined in a second-order scheme', *J. Comp. Phys.*, **14**, 361–370 (1974).
8. B. Van Leer, 'Towards the ultimate conservative differencing scheme V: A second-order sequel to Godunov's method', *J. Comp. Phys.*, **23**, 101–136 (1977).
9. P.K. Sweby, 'High resolution schemes using flux limiters for hyperbolic conservation laws', *SIAM J. Numer. Anal.*, **21**, 995–1011 (1984).
10. B.P. Leonard, 'Simple high-accuracy resolution program for convective modeling of discontinuities', *Int. J. Numer. Methods Fluids*, **8**, 1291–1318 (1988).
11. P.H. Gaskell and A.K.C. Lau, 'Curvature-compensated convective transport: SMART, a new boundedness-preserving transport algorithm', *Int. J. Numer. Methods Fluids*, **8**, 617–641 (1988).
12. M.S. Darwish, 'A new high-resolution scheme based on the normalized variable formulation', *Numer. Heat Transf. B*, **24**, 353–371 (1993).
13. T. Theodoropoulos, 'Prediction of three-dimensional engine flow on unstructured meshes', *Ph.D. Thesis*, Imperial College, University of London, 1990.
14. J.H. Ferziger and M. Perić, *Computational Methods for Fluid Dynamics*, Springer, Berlin, 1995.
15. A.D. Gosman, 'Developments in industrial computational fluid dynamics', *Trans. I. Chem. E.*, **76**, 153–161 (1998).
16. H. Jasak, 'Error analysis and estimation in the finite volume method with applications to fluid flows', *Ph.D. Thesis*, Imperial College, University of London, 1996.
17. S. Muzaferija and D. Gosman, 'Finite-volume CFD procedure and adaptive error control strategy for grids of arbitrary topology', *J. Comp. Phys.*, **138**, 766–787 (1997).
18. R.F. Warming and R.M. Beam, 'Upwind second-order difference schemes and applications in aerodynamic flows', *AIAA J.*, **14**, 1241–1249 (1976).
19. B.P. Leonard, 'A stable and accurate convective modelling procedure based on quadratic upstream interpolation', *Comp. Methods Appl. Mech. Eng.*, **19**, 59–98 (1979).
20. M.S. Darwish and F. Moukalled, 'Normalized variable and space formulation methodology for high-resolution schemes', *Numer. Heat Transf. B*, **26**, 79–96 (1994).
21. J. Zhu, 'A low-diffusive and oscillation-free scheme', *Commun. Appl. Numer. Methods*, **7**, 225–232 (1991).
22. STAR-CD Version 2.1—Manuals, Computational Dynamics Limited, 1991.
23. J. Zhu and W. Rodi, 'A low dispersion and bounded convection scheme', *Comp. Methods Appl. Mech. Eng.*, **92**, 87–96 (1991).
24. I. Demirdžić, M. Perić and Ž. Lilek, 'A collocated finite volume method for predicting flows at all speeds', *Int. J. Numer. Methods Fluids*, **16**, 1029–1050 (1993).